Available online at www.sciencedirect.com
SCIENCE DIRECT®
Catalysis Today 93–95 (2004) 135–140
CATALYSIS TODAY
www.elsevier.com/locate/cattod

n-Heptane isomerization over mesoporous MoO_x and Ni–MoO_x catalysts

Xinping Wang [a,*], Can Li [b], Yingjun Wang [a], Tian-Xi Cai [a]

[a] *State Key Laboratory of Fine Chemicals, Dalian University of Technology, Dalian, China*
[b] *State Key Laboratory of Catalysis, Dalian Institute of Chemical Physics, The Chinese Academy of Sciences, Dalian, China*

Abstract

MoO_x and Ni–MoO_x catalysts with maximum pore diameter at ca. 4.1 nm in the meso-pore range were prepared by reducing MoO_3 or NiO doped MoO_3 in H_2 flow at 623 K in a period of 6–12 h. The catalysts were used in *n*-heptane isomerization isothermally carried out at 573 K under atmospheric pressure in a conventional fixed-bed flow reactor. MoO_x is predominantly composed of the MoO_xH_y and MoO_2 phase. The former can be considered to be more active than the latter. Over the MoO_x catalyst, the H_2 partial pressure positively affected the reaction rate with an order of ca. 0.35. It can be deduced from the result that the MoO_x catalyst lacks active sites with a metallic character for dehydrogenation–hydrogenation step in *n*-heptane isomerization. The Ni–MoO_x catalysts have a lower specific surface area than the MoO_x catalysts, due to that the reduction of MoO_3 was accelerated by nickel, and the fact that more H_2O was produced in the initial reduction process, this leading to MoO_x sintering. Comparing with MoO_x catalysts, the 5% Ni–MoO_x catalysts are more active in terms of the reaction rate per unit surface area of the catalyst, the explanation is that the dehydrogenation–hydrogenation step in *n*-heptane isomerization is effectively enhanced by incorporation of Ni in the catalysts.

Keywords: MoO_x; Ni–MoO_x; Meso-pore; Isomerization; *n*-Heptane

1. Introduction

Environmental considerations have brought about a rapid phase out of lead additives and a braking of MTBE in gasoline in the recent years. It makes industrial isomerization processes converting linear alkanes into branched ones increasingly more important, because this processes offer a route to achieve high octane number of gasoline. Recently, molybdenum oxides (MoO_x) treated in H_2 at 623–673 K have attracted much attention because of their high catalytic activity and selectivity for *n*-heptane isomerization. Matsuda et al. have reported that MoO_x with a maximum porosity around 0.6 nm in diameter obtained by a 12 h or longer period H_2 reduction of MoO_3 at 623 K was more active and selective for isomerization of *n*-heptane, compared with 0.5 wt.% Pt/USY zeolite. They have suggested that the MoO_x possesses bifunctional properties, which are responsible for the higher isomerization activity [1–4]. In this paper, we report on MoO_x and Ni–MoO_x catalysts with maximum pore volume in the meso-pore range used in the *n*-heptane isomerization reaction.

2. Experimental

2.1. Catalyst preparation

The MoO_3 used in this study was a commercial powder (Beijing Chemicals) with Analytical Purity. After being compressed into pellets, and crushed, 0.15 g of the sample (60–80 mesh) of pure MoO_3 or doped with nickel oxide (NiO–MoO_x) was charged into a stainless steel reactor with a diameter of 3.8 mm, reduced by H_2 (which was purified by passing through a Pd/Al_2O_3 catalyst and then dried with 3A molecular sieve on line). In the reduction process, the temperature was first raised from 373 to 623 K at the rate of 5 K min^{-1} and then held at the reduction temperature for a desired period with H_2 flow of 120 ml min^{-1}. To obtain the catalyst sample for characterizations, the catalyst, protected

* Corresponding author.
E-mail address: wangxp.wuhua@263.net (X. Wang).

0920-5861/$ – see front matter © 2004 Published by Elsevier B.V.
doi:10.1016/j.cattod.2004.06.033

by N_2, was cooled to room temperature and then passivated for 3 h with a gas mixture containing 0.5% O_2 in N_2 to avoid bulk oxidation. The catalysts were denoted by the Ni percent in the precursors that were submitted to activation by the reduction, and the reduction period. For instance, MoO_3(2) represents the catalyst obtained by reducing MoO_3 in H_2 for 2 h, and 5% Ni–MoO_3(6) denotes that the catalyst obtained from a NiO–MoO_3 precursor with Ni/(Ni + Mo) molar ratio 5%, reduced in H_2 for 6 h.

2.2. Catalyst characterization

Crystalline phases of the catalysts were characterized in Riguka D/max 2400 X-ray diffractometer using Cu Kα radiation under 40 kV and 100 mA. To evaluate the percentage of MoO_3 retained in the MoO_3(2) catalyst, a set of mechanically mixed samples containing different amounts of MoO_3 and MoO_3(12) were determined by XRD in uniform analyzing conditions. BET surface area and pore size distribution of the catalysts were determined at liquid nitrogen temperature by a Micrometritics ASAP-2000 adsorption analyzer.

2.3. Catalytic activity measurement

The isomerization of *n*-heptane was isothermally carried out at 573 K under atmospheric pressure in a conventional fixed-bed flow reactor. The catalyst being submitted to the activity measurement was prepared in situ without undergoing passivation. The reactant gas containing *n*-heptane, H_2, and N_2 (as complement gas) was fed in the reactor downwards with a total flow rate 125.3 ml min^{-1}. The composition of effluent gas was analyzed by means of FID gas chromatography using quartz capillary separation column. The selectivity to *iso*-C_7 was defined as the ratio of *iso*-C_7 products to *n*-C_7 transformed in terms of moles.

3. Results and discussion

3.1. The MoO_x catalysts

The physico-chemical structure of MoO_x catalysts obtained by reducing MoO_3 in H_2 at 623 K for different period were characterized in their bulk and surface properties. As shown in Fig. 1, almost all MoO_3 in sample MoO_3(2) is reduced by hydrogen, though the diffraction lines ($2\theta = 12.7^\circ$, 25.42°, 38.48°) corresponding to MoO_3 phases are still detected. It was determined quantitatively by the XRD method that less than 1/30 of molybdenum maintained the original MoO_3 phase in the MoO_3(2) sample. In the MoO_3(6) sample, the diffraction lines of MoO_3 phases completely disappear. The sample consists of MoO_2 and some phases with diffraction lines at $2\theta = 14.4^\circ$ ($d = 0.6137$ nm), $2\theta = 29.3^\circ$ ($d = 0.3048$ nm), $2\theta = 38.3^\circ$ ($d = 0.2346$ nm), and $2\theta = 44.4^\circ$ ($d = 0.2037$ nm). This indicates that MoO_3 can be easily reduced by H_2 at 623 K in our reduction conditions. In the XRD diagrams, it seems that the diffraction lines at $2\theta = 14.4^\circ$ and 29.3° diminish simultaneously when the reduction period is prolonged. Taking account of that the *d*-value 0.6137 nm of the former is almost equal to the double of that of the latter, it is suggested that both diffractions belong to the same crystalline phase H_xMoO_3. On the other hand, the two diffraction lines at 38.3° and 44.4°, being hardly changed in intensity when the reduction period increases, can be considered to be derived from a MoO_xH_y phase. Leclercq and co-workers reported that MoO_xC_y prepared by the decomposition of $Mo(CO)_6$ gave diffraction lines at $2\theta = 38^\circ$ and 44° [5,6]. Delporte et al. [7] stated that a treatment of MoO_3 with a mixture of H_2 and hydrocarbon at 623 K yielded the MoO_xC_y phase, and that hydrogen was able to act like carbon atoms to form MoO_xH_y, of which the diffraction line appeared at $2\theta = 44.3^\circ$. Matsuda et al. also suggested that the two peaks at $2\theta = 38.1^\circ$ and 44.3° were associated with the formation of the MoO_xH_y phase. Although the diffraction lines at $d = 0.6137$ nm ($2\theta = 14.4^\circ$), $d = 0.3048$ nm ($2\theta = 29.3^\circ$) and $d = 0.2037$ nm ($2\theta = 44.4^\circ$) in Fig. 1 are very close to those $d = 0.6198$, 0.3057, and 0.2038 nm of the $Mo_xO_yC_z$ phase reported by Ledoux et al. [8], the presence of a carbon-containing phase can be excluded here, since the reduction process was carefully controlled to be free of hydrocarbons in our experiments. In favor of this conclusion is the fact that the catalyst sample MoO_3(1) which was obtained by one hour's hydrogen-reduction of MoO_3 at 623 K and then submitted to *n*-heptane isomerization for 1 h at the same temperature, did not show a stronger intensity of the three peaks than those of MoO_x sample as-prepared by pure H_2 reduction, as shown in Fig. 1. This shows that carbon is not incorporated in the sample even in more favorable conditions.

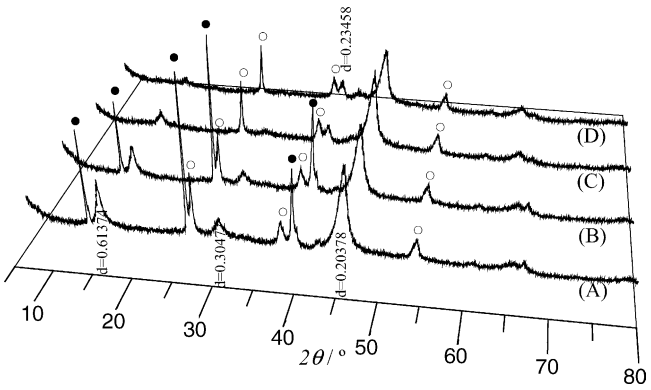

Fig. 1. XRD patterns of MoO_x obtained by reducing MoO_3 in H_2 at 623 K for different periods: (A) 2 h; (C) 6 h; (D) 12 h; (B) 1 h (which was then submitted to *n*-heptane isomerization reaction for 1 h). (●) Peaks corresponding to MoO_3; (○) MoO_2.

From Fig. 1, it can be also observed that the relative intensity of the diffractions due to the MoO_xH_y and MoO_2 phases are almost unchanged irrespective of the reduction period, indicating that both phases in the MoO_x catalysts were formed simultaneously in the reduction process of

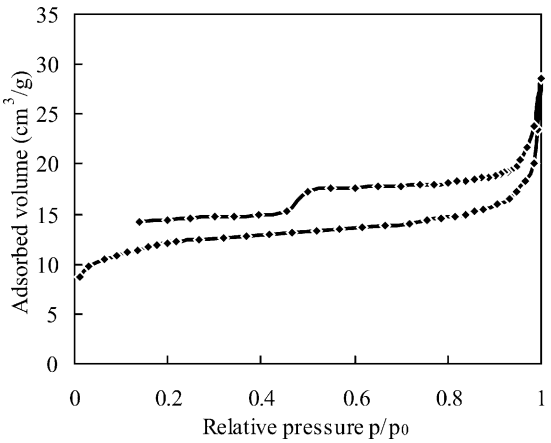

Fig. 2. Adsorption–desorption isotherms of N_2 on MoO_3(12 h).

MoO_3. Compared with the XRD patterns that presented by Matsuda et al. in literature [2,9], MoO_x(12 h) shows a stronger diffraction intensity of those due to MoO_xH_y and a weaker intensity of MoO_2, indicating that the MoO_x(12 h) catalyst contains more MoO_xH_y phases and less MoO_2 phases than that reported by the authors [1,2,9].

The physical structure of the MoO_x catalysts in our study markedly differs from that mentioned in literature data, in which some MoO_x samples with surface area of 170–180 $m^2\,g^{-1}$ and with a maximum pores volume at diameter of ca. 0.6 nm were reported [2,9]. Concerning all the MoO_x catalysts we tested, the BET equation provided satisfactory linear fit of the N_2 adsorption data. This gave BET surface areas of 36.2 and 41.6 $m^2\,g^{-1}$ for MoO_3(6) and MoO_3(12), respectively. The MoO_x catalysts exhibited obvious N_2 adsorption–desorption hysteresis in the relative pressure, p/p_0, in the range of ca. 0.5–0.9985. The hysteresis on MoO_3(12) is displayed in Fig. 2. The corresponding pore-size distribution curve (Fig. 3) being calculated on the basis of the N_2 desorption data shows a maximum pore volume diameter at ca. 4.1 nm in meso-pore range.

In recent years, the surface area of MoO_3 has been extensively reported to be enlarged after a temperature-programmed reaction with NH_3 [10–13], carburization under H_2 and hydrocarbon mixtures [7,14,15], and in H_2 reduction [7].

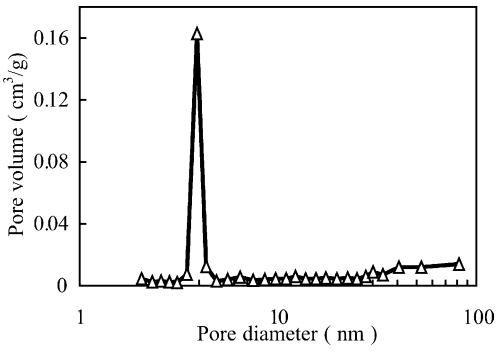

Fig. 3. Pore-size distribution for MoO_3(12 h).

The following mechanism has been proposed to explain the results: The reduction of MoO_3 begins preferentially at the crystallographic defects, and as the reduction proceeds, the contraction of lattice fractures the crystal wherein [16]. According to this mechanism, the measured meso-pores characterized by the N_2 adsorption–desorption hysteresis can be considered as reflecting the clearance between some uniform nano-particles of MoO_x being formed as a consequence of crystal rupture. This suggestion may also be supported by the fact that the MoO_x samples do not present small angle X-ray scattering (SAXS) being characteristic of regular meso-pore structure similar to that of meso-pore molecule sieves, as shown in Fig. 1.

The activity of the MoO_x catalysts for *n*-heptane isomerization at 573 K strongly depends on the reduction period. As shown in Fig. 4, *n*-heptane conversion sharply increased with the reduction period of the catalyst in the first hours and then reached a constant value when the reduction period was prolonged to 12 h. The changes in catalyst activity versus the reduction period are quite consistent with the considerable modification in the bulk composition of MoO_x illustrated in Fig. 1, observed within the reduction period of 12 h, especially in the first 6 h. The MoO_x(12 h) catalyst gave 50.3% conversion of *n*-heptane in the following conditions: $W/F = 11.0\,g_{cat}\,h\,mol\,C_7^{-1}$, and H_2/*n*-heptane = 23 (in volume ratio). In Ref. [1], an *n*-heptane conversion of 46.1% in the conditions of 12.5 $g_{cat}\,h\,mol\,C_7^{-1}$ of *W*/*F*, 40 of H_2/*n*-heptane ratio in volume, at 573 K was achieved over a MoO_x(24 h) catalyst with a specific surface area 47.9 $m^2\,g^{-1}$ obtained by 24 hours' hydrogen reduction of MoO_3. Taking the differences of reaction conditions into account, it seems that the MoO_x(12 h) catalyst with a specific surface area 41.6 $m^2\,g^{-1}$ being composed of more MoO_xH_y phases and less MoO_2 phases has higher activity in unit surface for the *n*-heptane isomerization, in comparison with the MoO_x(24 h) catalyst mentioned in literature [1]. From these results, it can be deduced that the MoO_xH_y phase is more

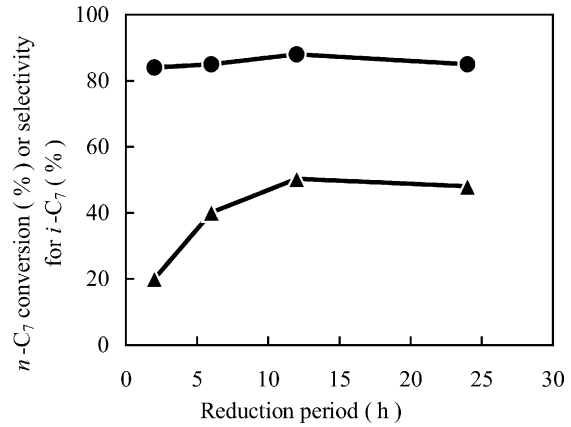

Fig. 4. The catalytic activity of MoO_x for *n*-heptane isomerization prepared in different reduction period at 623 K ((▲) *n*-C_7 conversion; (●) selectivity for *i*-C_7). Reaction conditions: $T = 573$ K, H_2/*n*-C_7=25; $W/F = 11\,g_{cat}\,h\,mol^{-1}$.

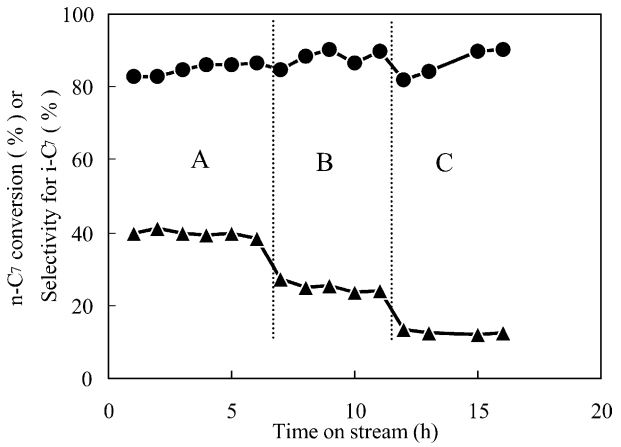

Fig. 5. The dependence of *n*-heptane conversion on partial pressure of H_2: (▲) *n*-C_7 conversion; (●) selectivity for *i*-C_7. (A) $p_{H_2} = 97.0$ kPa, (B) $p_{H_2} = 48.5$ kPa, (C) $p_{H_2} = 24.2$ kPa. Reaction conditions: $T = 573$ K, $W/F = 11\ g_{cat}\ h\ mol^{-1}$, total flow rate $= 125.3\ ml\ min^{-1}$.

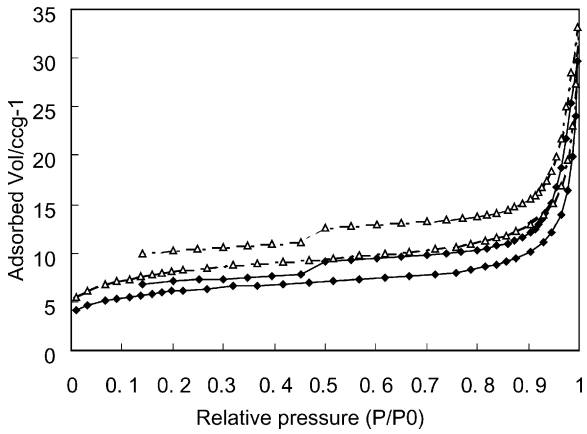

Fig. 6. The adsorption–desorption isotherms of N_2 on Ni–MoO_3 catalysts: (◆) Ni–MoO_3(6 h) (△) Ni–MoO_3(12 h).

active for *n*-heptane isomerization than the MoO_2 phase. In some previous investigations [17,18], this has to be noticed, it seems that the role of the MoO_2 phase in alkane isomerization has been strongly emphasized by the researchers.

Taking notice of the difference with respect to the H_2/*n*-heptane ratio used in *n*-heptane isomerization between that in our research and that in the literature, the influence of H_2 partial pressure on the reaction was investigated. The effect of H_2 partial pressure is illustrated in Fig. 5. In reaction conditions where we kept constant the *n*-heptane feed, and the total flow rate of the reactant gas mixture (including complementary gas of N_2) to be $125.3\ ml\ min^{-1}$, the *n*-heptane conversion over MoO_x(6 h) catalyst exhibits a sharp decline with the decrease of the H_2 partial pressure, indicating that the H_2 partial pressure exerts a positive contribution to *n*-heptane isomerization. This implies that the conversion of *n*-heptane would be much higher than 50.3%, over the MoO_x(6 h) catalyst if the reaction proceeded at the H_2/*n*-heptane ratio of 40 that was used in literature [1].

From Fig. 5, a reaction order of 0.35 with respect to H_2 partial pressure in the *n*-heptane isomerization over the MoO_3(6 h) catalyst was obtained, by plotting ln(*FC*) versus $\ln p_{H_2}$, where *F*, *C* and p_{H_2} denote the flow rate of *n*-heptane, its conversion, and partial pressure of H_2, respectively. It differs from the Pd/SAPO-11 catalyst [19] and the oxygen-modified molybdenum carbide catalyst [20], over which negative reaction orders for H_2 partial pressure were obtained. Comparing to classical bifunctional catalysts, the MoO_x catalyst seems to possess more acidic sites active for isomerization step and less active sites with a metallic character for the dehydrogenation–hydrogenation step, if we take into account the bifunctional properties of MoO_x [1].

3.2. The 5% Ni–MoO_x catalysts

Nickel is well known as an effective component of catalyst in reaction involving H_2 activation. To improve the metallic function of MoO_x in the *n*-heptane isomerization, nickel doped MoO_x catalysts were investigated. The 5% Ni–MoO_x catalysts give also satisfactory linear BET relation and evident hysteresis with respect to the N_2 relative pressure, as shown in Fig. 6. Although the 5% Ni–MoO_x catalysts had been prepared by hydrogen reduction in the same way as that of the MoO_x catalysts, they unfortunately exhibited a specific BET surface area of only 21.4 and 28.6 $m^2\ g^{-1}$ for the 5% Ni–MoO_x(6 h) and 5% Ni–MoO_x(12 h), respectively, which is obviously less than that of the counterpart of the MoO_x catalysts. On the other hand, the 5% Ni–MoO_x catalysts have the same maximum pore diameter ca. 4.1 nm as that of the MoO_x catalysts, as shown in Fig. 7.

The chemical bulk properties of the 5% Ni–MoO_x catalysts are reported in Fig. 8. Comparing with MoO_x catalysts, the 5% Ni–MoO_x catalysts seems to have less MoO_2 phases (corresponding to the diffractions at $2\theta = 26.1°$, 37.0°, 53.6°), in comparison to the MoO_xH_y phases. Tt can also be observed that the nickel oxide doped MoO_3 was more easily reduced by H_2 than pure MoO_3 at 623 K. Whereas the sample still contained about 1/30 of MoO_3 when it was reduced for 2 h in the case of MoO_x(2 h), no MoO_3 phase was detectable in the case of 5% Ni–MoO_x(2 h). The promotion due to the nickel component for the MoO_3 reduction may be attributed to its effective function for H_2 activation. The promotion may also concern the *n*-heptane isomerization results. For example, the catalyst prepared by hydrogen reduction of MoO_3 for 12 h at 573 K, provided only 7.5% of the *n*-heptane conversion, while on the catalyst prepared from nickel oxide (5 wt.%) doped MoO_3 in the same reduction conditions, 27.5% of *n*-heptane conversion was achieved.

It was reported that Mo_2N with larger surface area was synthesized in temperature-programmed reaction of MoO_3 and NH_3. The resultant high surface area was achieved only when the reaction took place at a slow, controlled rate and in a greater space velocity of NH_3 [16,21]. The reason suggested by the authors was that, the presence of H_2O vapor produced by the reduction might cause sintering of the prod-

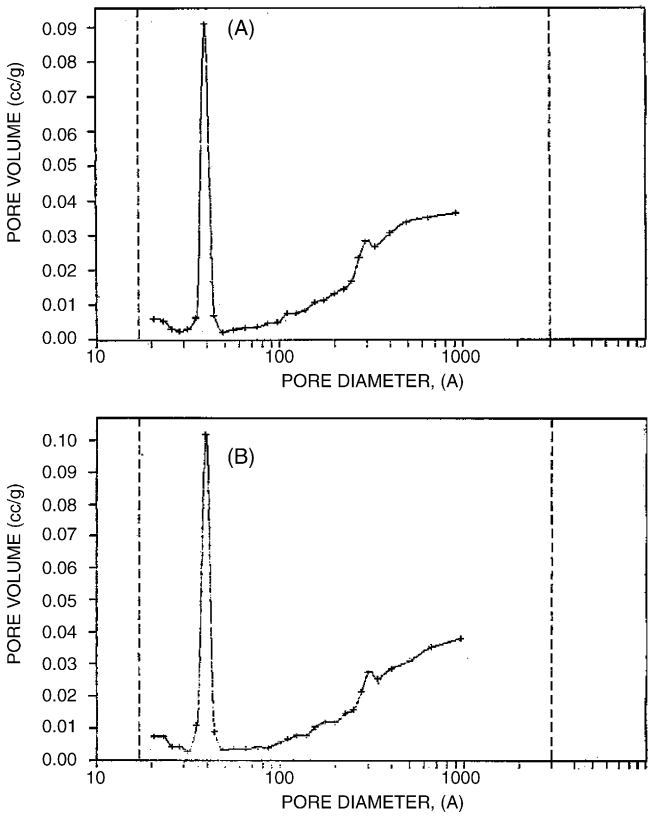

Fig. 7. Pore-size distributions for Ni–MoO_x catalysts: (A) Ni–MoO_x(6 h), (B) Ni–MoO_x(12 h).

uct Mo_2N. The favorable effect was supposed to be due to the fact that the partial pressure was lowered in the conditions of slow reduction rate and large flow rate of the reactive gas [16]. Recently, Matsuda et al. in some experiments further confirmed the suggestion. They found that the surface area of MoO_x was strongly influenced by the partial pressure of H_2O mixed with the reactive gas H_2 [9]. In the case of Ni–MoO_x catalysts, the reduction of MoO_3 is accelerated by the nickel component, and the increased production of H_2O in the initial reduction steps leads to MoO_x sintering, so that Ni–MoO_x sample with less surface area than that of MoO_x is obtained.

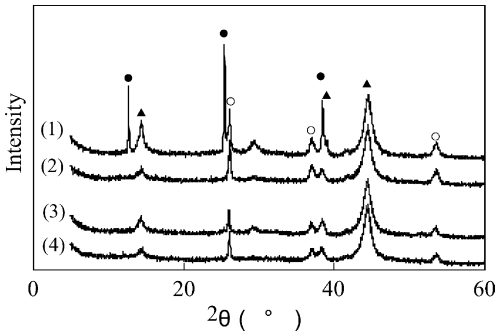

Fig. 8. XRD patterns of MoO_x and Ni–MoO_x catalysts reduced in different periods (1) MoO_x reduced for 2 h, (2) for 6 h, (3) Ni–MoO_x reduced for 2 h, (4) for 6 h, corresponding to MoO_3 (●), MoO_2 (○), MoO_xH_y (▲).

The catalytic performance of the 5% Ni–MoO_x catalysts in *n*-heptane isomerization is summarized in Table 1. The 5% Ni–MoO_x catalysts are not superior to the counterpart MoO_x catalysts when activity in per gram in *n*-heptane isomerization is considered, due to their lower specific surface areas. However, in terms of reaction rate per unit surface area, all the 5% Ni–MoO_x catalysts have a higher activity than the MoO_x catalysts in the same reaction conditions. Nevertheless, from the view point of catalysis, it remains still not clear whether the nickel component is favorable for *n*-heptane isomerization or not. The reason is that the 5% Ni–MoO_x and MoO_x catalysts contain different percentages of MoO_xH_y phase. To further evaluate the effect of nickel component in the catalytic *n*-heptane isomerization, 0.133 g of a mechanical mixture, composed of 0.13 g of MoO_x(6 h) (which corresponds to 0.15 g of MoO_3, assuming that all of molybdenum in MoO_x exists as MoO_2) and 0.003 g of nickel metal powder, had been pressed into 60–80 mesh, and was tested as catalyst in the same reaction conditions. As shown in Table 1, the mixture provides 51.8% of *n*-heptane conversion, after being pretreated in H_2 at 573 K for half an hour. This indicates that, in the case of 5% Ni–MoO_x, the addition of NiO to MoO_3 is not only in favor of the MoO_xH_y phases formation in the reduction process, but also facilitates *n*-heptane isomerization, by activating H_2 and therefore enhancing the dehydrogenation–hydrogenation step in

Table 1
Catalytic performance of the 5% Ni–MoO_x catalysts compared with MoO_x

Catalyst	BET surface (m^2/g)	Conversion of *n*-C_7 (%)	Relative activity on unit surface area[b]	Selectivity to *n*-C_7 (%)
MoO_x(2 h)	–[a]	20.0	–[a]	84
MoO_x(6 h)	36.1	40.1	1	85
MoO_x(12 h)	41.6	50.3	1.1	88
5% Ni–MoO_x(2 h)	–[a]	30.9	–[a]	87
5% Ni–MoO_x(6 h)	21.4	43.6	1.8	86
5% Ni–MoO_x(12 h)	28.6	45.3	1.4	80
5% Ni + MoO_x(6 h)	–[a]	51.8	1.3[c]	82

[a] Not measured, or calculated.
[b] Relative to that of MoO_x(6 h) which defined activity unit.
[c] Calculated by assuming that the Ni powder does not provide surface area and that all molybdenum in MoO_x existed as MoO_2.

n-heptane isomerization over MoO_x. Of course, the diminution of the catalyst surface area and decrease of selectivity to *n*-heptane isomerization in the reaction owing to the addition of nickel are not satisfactory. These disadvantages might probably overcome by activating the catalyst at lower reduction temperature and using it at lower reaction temperature, respectively.

4. Conclusion

MoO_x catalysts with maximum pore volume diameter at ca. 4.1 nm in meso-pore range can be obtained by reducing MoO_3 in H_2 flow at 623 K over a period of 6–12 h. The meso-pores characterized by the N_2 adsorption–desorption hysteresis can be considered as reflecting the clearance between uniform nano-particles of MoO_x being formed as a consequence of the crystal rupture of MoO_3.

The MoO_x is predominantly composed of MoO_xH_y phase and MoO_2 phase, and the former phase can be considered to be more active than the latter one for *n*-heptane isomerization. Over the MoO_x catalyst, the H_2 partial pressure positively affects the reaction rate with an order of ca. 0.35, therefore it can be deduced from the result that the MoO_x catalyst lacks active sites for dehydrogenation–hydrogenation step in *n*-heptane isomerization.

By incorporation of NiO into MoO_3, Ni–MoO_x catalysts with maximum pore volume diameter at ca. 4.1 nm can be obtained in the same way as for the MoO_x catalysts. The Ni–MoO_x catalysts thus obtained have a specific surface area lower than the MoO_x catalysts, because the reduction of MoO_3 is accelerated by the nickel component, and more H_2O is produced in the initial reduction process, this leading to MoO_x sintering. Comparing with MoO_x catalysts, the 5% Ni–MoO_x catalysts are more active in terms of the reaction rate per unit surface area of the catalyst. The explanation is that the dehydrogenation–hydrogenation step in *n*-heptane isomerization is effectively enhanced by the incorporation of Ni in the catalysts.

References

[1] T. Matsuda, H. Shiro, H. Sakagami, N. Takahashi, Catal. Lett. 47 (1997) 99–103.
[2] T. Matsuda, Y. Hirata, H. Itoh, H. Sakagami, N. Takahashi, Micropor. Mesopor. Mater. 42 (2001) 337–344.
[3] T. Matsuda, H. Sakagami, N. Takahashi, Appl. Catal. A: Gen. 213 (2001) 83–90.
[4] T. Matsuda, A. Hanai, F. Uchijima, H. Sakagami, N. Takahashi, Micropor. Mesopor. Mater. 51 (2002) 155–164.
[5] L. Leclercq, K. Imura, S. Yoshida, T. Barbee, M. Boudart, Stud. Surf. Sci. Catal. 3 (1979) 627–639.
[6] M. Boudart, S.T. Oyama, L. Leclercq, in: T. Seiyama, K. Tanabe (Eds.), Proceedings of the Seventh ICC, vol. 1, Tokyo, Elsevier, Amsterdam, 1980, 578 pp.
[7] P. Delporte, F. Meunier, C. Pham-Huu, P. Vennegues, M.J. Ledoux, J. Guille, Catal. Today 23 (1995) 251–267.
[8] M.J. Ledoux, C. Pham-Huu, P. Delporte, E.A. Blekkan, A.P.E. York, Stud. Surf. Sci. Catal. 92 (1994) 81–86.
[9] T. Matsuda, Y. Hirata, F. Uchijima, H. Itoh, N. Takahashi, Bull. Chem. Soc. Jpn. 73 (2000) 1029–1034.
[10] L. Volpe, M. Boudart, J. Solid State Chem. 59 (1985) 332–347.
[11] K.S. Lee, H. Abe, J.A. Reimer, A.T. Bell, J. Catal. 139 (1993) 34–40.
[12] R.S. Wise, E.J. Markel, J. Catal. 145 (1994) 344–355.
[13] J.G. Choi, R.L. Curl, L.T. Thompson, J. Catal. 146 (1994) 218–227.
[14] Y. Sato, D. Imai, A. Sato, S. Kasahara, K. Omata, M. Yamada, Sekiyo Gakkaishi 37 (1994) 514–521.
[15] J.S. Lee, S.T. Oyama, M. Boudart, J. Catal. 106 (1987) 125–133.
[16] E.J. Markel, J.W. Van Zee, J. Catal. 126 (1990) 643–657.
[17] A. Karrib, V. Logie, N. Saurel, P. Wehrer, L. Hilaire, G. Maire, Surf. Sci. 377–379 (1997) 754–758.
[18] A. Karrib, D. Mey, G. Maire, Catal. Today 65 (2001) 179–183.
[19] M. Höchtl, A. Jentys, H. Vinek, J. Catal. 190 (2000) 419–432.
[20] E.A. Blekkan, C. Pham-Huu, M.J. Ledoux, J. Guille, Ind. Eng. Chem. Res. 33 (1994) 1657–1664.
[21] S.T. Oyama, J.C. Schlatter, J.E. Metcalf Jr., J.M. Lambert Jr., Ind. Eng. Chem. Res. 27 (1988) 1639–1648.